

Hyper Spectral Image Segmentation of Land Resources Classification Based Kernel Classifier

^[1] Nandhini Devi.V, ^[2] Ahila.A
^[1] M.E&ECE, ^{[1][2]} IJCE keelavallanadu, Tuticorin

Abstract: - For the classification of hyper spectral images (HSIs), this work presents a novel framework for an automatic system to segment the hyper spectral images. In the HSI, each pixel can be regarded as a shape-adaptive region, which consists of a number of spatial neighboring pixels with very similar spectral characteristics. First, the proposed methodology adopts an over segmentation algorithm to cluster the HSI into many super pixels. Then, feature extraction is employed for the utilization of the spectral information, as well as spatial information, within and among super pixels. Finally, the hybridized machine learning algorithm is incorporated for the hyper spectral classification. This work introduces particle swarm optimization based support vector machine classifier for the classification. The Pavia database images are collected and simulated on MATLAB R2014a and the exposed results are showing the effectiveness of the proposed methodology.

I. INTRODUCTION

Hyper spectral imaging, like other spectral imaging, collects and processes information from across the electromagnetic spectrum. The goal of hyper spectral imaging is to obtain the spectrum for each pixel in the image of a scene, with the purpose of finding objects, identifying materials, or detecting processes. Nowadays there are two branches of spectral imaging Push broom scanner, which read in an image over time and Snapshot hyper spectral imaging which generates an image in an instance.

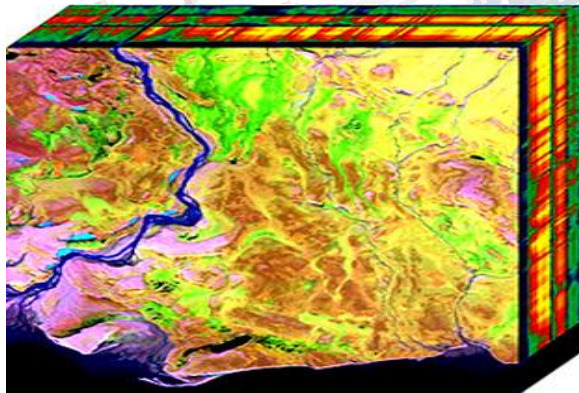


Figure 1.1 Two-dimensional projection of a hyper spectral cube

Whereas the human eye sees color of visible light in mostly three bands (red, green, and blue), spectral imaging divides the spectrum into many more bands. This technique of dividing images into bands can be extended

beyond the visible. In hyperspectral imaging, the recorded spectra have fine wavelength resolution and cover a wide range of wavelengths.

Engineers build hyperspectral sensors and processing systems for applications in astronomy, agriculture, biomedical imaging, geosciences, physics, and surveillance. Hyperspectral sensors look at objects using a vast portion of the electromagnetic spectrum. Certain objects leave unique 'fingerprints' in the electromagnetic spectrum. Known as spectral signatures, these 'fingerprints' enable identification of the materials that make up a scanned object. For example, a spectral signature for oil helps geologists find new oil fields. Figuratively speaking, hyperspectral sensors collect information as a set of 'images'. Each image represents a narrow wavelength range of the electromagnetic spectrum, also known as a spectral band. These 'images' are combined to form a three-dimensional (x,y,λ) hyperspectral data cube for processing and analysis, where x and y represent two spatial dimensions of the scene, and λ represents the spectral dimension (comprising a range of wavelengths).

Technically speaking, there are four ways for sensors to sample the hyperspectral cube: Spatial scanning, spectral scanning, snapshot imaging and spatio-spectral scanning.

Hyperspectral cubes are generated from airborne sensors like the NASA's Airborne Visible/Infrared Imaging Spectrometer (AVIRIS), or from satellites like NASA's EO-1 with its hyperspectral instrument Hyperion. However, for many development and validation studies, handheld sensors are used. The precision of these sensors is typically measured in spectral resolution, which is the width of each band of the spectrum that is captured. If the scanner detects a large number of fairly narrow frequency bands, it is

possible to identify objects even if they are only captured in a handful of pixels. However, spatial resolution is a factor in addition to spectral resolution. If the pixels are too large, then multiple objects are captured in the same pixel and become difficult to identify. If the pixels are too small, then the energy captured by each sensor cell is low, and the decreased signal-to-noise ratio reduces the reliability of measured features. The acquisition and processing of hyperspectral images is also referred to as imaging spectroscopy or, with reference to the hyperspectral cube, as 3D spectroscopy. For feature dimension reduction, another approach is to perform band selection which aims to select a group of bands from the original high-dimensional feature space. The correlation between each two spectral bands is measured by mutual information, and the representative bands are selected by minimizing the distance between the selected bands and the estimated reference map. Then the representative bands are selected by using a clustering-based method in which the bands with the largest similarity to other bands are chosen. For hyperspectral image classifiers, K-Nearest Neighbor classifier (KNN) and Support Vector Machine (SVM) have been employed.

II - RELATED WORK

In [1], J. M. Bioucas-Dias et al., proposed segmentation approach is experimentally evaluated using both simulated and real hyperspectral data sets, exhibiting state-of-the-art performance when compared with recently introduced hyperspectral image classification methods. The integration of subspace projection methods with the MLR algorithm, combined with the use of spatial-contextual information, represents an innovative contribution in the literature. This approach is shown to provide accurate characterization of hyperspectral imagery in both the spectral and the spatial domain. L. Bruzzone, et al., [3] propose a theoretical discussion and experimental analysis aimed at understanding and assessing the potentialities of SVM classifiers in hyper dimensional feature spaces. Then, we assess the effectiveness of SVMs with respect to conventional feature-reduction-based approaches and their performances in hyper subspaces of various dimensionalities. To sustain such an analysis, the performances of SVMs are compared with those of two other nonparametric classifiers (i.e., radial basis function neural networks and the K-nearest neighbor classifier). M. Fauvel, et al., [4] proposed scheme is a spectral-spatial technique based on wavelet transforms and mathematical morphology. The original contribution of this paper is that the extended morphological profile (EMP) is created from the features extracted by wavelets, which has proven to be better or comparable to other techniques for dimensionality

reduction of hyperspectral data. X. Huang et al., [5] introduce a novel feature extraction algorithm named sparse transfer manifold embedding (STME), which can effectively and efficiently encode the discriminative information from limited training data and the sample distribution information from unlimited test data to find a low-dimensional feature embedding by a sparse transformation. Technically speaking, STME is particularly designed for hyperspectral target detection by introducing sparse and transfer constraints.

III - PROPOSED SYSTEM

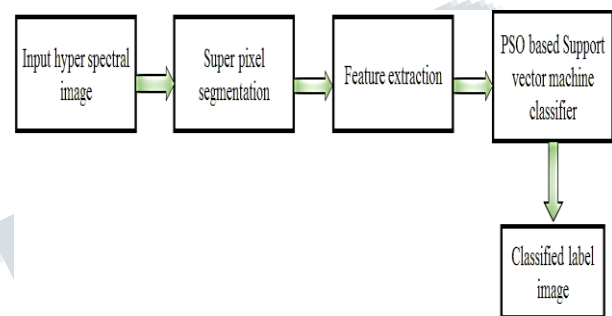


Fig 3.1 proposed block

A. SUPER PIXEL SEGMENTATION

Superpixels provide a convenient primitive from which to compute local image features. They capture redundancy in the image and greatly reduce the complexity of subsequent image processing tasks. They have proved increasingly useful for applications such as depth estimation, image segmentation, skeletonization, body model estimation, and object localization. For Superpixels to be useful they must be fast, easy to use, and produce high quality segmentations. Unfortunately, most state-of-the-art superpixel methods do not meet all these requirements.

B. SIMPLE LINEAR ITERATIVE CLUSTERING (SLIC)

This approach generates superpixels by clustering pixels based on their color similarity and proximity in the image plane. This is done in the five-dimensional [labxy] space, where [lab] is the pixel color vector in CIELAB color space, which is widely considered as perceptually uniform for small color distances, and xy is the pixel position. While the maximum possible distance between two colors in the CIELAB space (assuming sRGB input images) is limited, the spatial distance in the xy plane depends on the image size. It is not possible to simply use the Euclidean distance in this 5D space without normalizing the spatial distances. In order to cluster pixels in this 5D space, we therefore introduce a new distance measure that considers superpixel size. Using it, we enforce color similarity as well as pixel

proximity in this 5D space such that the expected cluster sizes and their spatial extent are approximately equal.

(a) Distance measure

Our algorithm takes as input a desired number of approximately equally-sized superpixels K . For an image with N pixels, the approximate size of each superpixel is therefore N/K pixels. For roughly equally sized superpixels there would be a superpixel center at every grid interval $S = \sqrt{N/K}$.

At the onset of our algorithm, we choose K superpixel cluster centers $C_k = [l_k, a_k, b_k, x_k, y_k]^T$ with $k = [1; K]$ at regular grid intervals S . Since the spatial extent of any superpixel is approximately S^2 (the approximate area of a superpixel), we can safely assume that pixels that are associated with this cluster center lie within a $2S \times 2S$ area around the superpixel center on the xy plane. This becomes the search area for the pixels nearest to each cluster center. Euclidean distances in CIELAB color space are perceptually meaningful for small distances (m in Eq. 1). If spatial pixel distances exceed this perceptual color distance limit, then they begin to outweigh pixel color similarities (resulting in superpixels that do not respect region boundaries, only proximity in the image plane). Therefore, instead of using a simple Euclidean norm in the 5D space, we use a distance measure D_s defined as follows:

$$d_{lab} = \sqrt{(l_k - l_i)^2 + (a_k - a_i)^2 + (b_k - b_i)^2}$$

$$d_{xy} = \sqrt{(x_k - x_i)^2 + (y_k - y_i)^2}$$

$$D_s = d_{lab} + \frac{m}{s} d_{xy}$$

Where D_s is the sum of the lab distance and the xy plane distance normalized by the grid interval S . A variable m is introduced in D_s allowing us to control the compactness of a superpixel. The greater the value of m , the more spatial proximity is emphasized and the more compact the cluster. This value can be in the range $[1; 20]$. We choose $m = 10$ for all the results in this paper. This roughly matches the empirical maximum perceptually meaningful CIELAB distance and offers a good balance between color similarity and spatial proximity.

(b) Algorithm

The simple linear iterative clustering algorithm is summarized in Algorithm 1. We begin by sampling K regularly spaced cluster centers and moving them to seed locations corresponding to the lowest gradient position in a 3×3 neighborhood. This is done to avoid placing them at an edge and to reduce the chances of choosing a noisy pixel. Image gradients are computed as:

$$G(x, y) = \|I(x + 1, y) - I(x - 1, y)\|^2 + \|I(x, y + 1) - I(x, y - 1)\|^2$$

Where $I(x, y)$ the lab is vector corresponding to the pixel at position (x, y) , and $\|\cdot\|$ is the L2 norm. This takes into account both color and intensity information. Each pixel in the image is associated with the nearest cluster center whose search area overlaps this pixel. After all the pixels are associated with the nearest cluster center, a new center is computed as the average lab $_{xy}$ vector of all the pixels belonging to the cluster. We then iteratively repeat the process of associating pixels with the nearest cluster center and recomputing the cluster center until convergence.

Algorithm 1 Efficient superpixel segmentation

- 1: Initialize cluster centers $C_k = [l_k, a_k, b_k, x_k, y_k]^T$ by sampling pixels at regular grid steps S .
- 2: Perturb cluster centers in an $n \times n$ neighborhood, to the lowest gradient position.
- 3: repeat
- 4: for each cluster center C_k do
- 5: Assign the best matching pixels from a $2S \times 2S$ square neighborhood around the cluster center according to the distance measure (Eq. 1).
- 6: end for
- 7: Compute new cluster centers and residual error E {L1 distance between previous centers and recomputed centers}
- 8: until $E < \text{threshold}$
- 9: Enforce connectivity.

At the end of this process, a few stray labels may remain, that is, a few pixels in the vicinity of a larger segment having the same label but not connected to it. While it is rare, this may arise despite the spatial proximity measure since our clustering does not explicitly enforce connectivity. Nevertheless, we enforce connectivity in the last step of our algorithm by relabeling disjoint segments with the labels of the largest neighboring cluster. This step is $O(N)$ complex and takes less than 10% of the total time required for segmenting an image.

C. SPECTRAL FEATURE EXTRACTION

Mean (or) Average filtering is a simple, intuitive and easy to implement method of smoothing images, i.e. reducing the amount of intensity variation between one pixel and the next. It is often used to reduce noise in images.

The idea of mean filtering is simply to replace each pixel value in an image with the mean ('average') value of its neighbors, including itself. This has the effect of eliminating pixel values which are unrepresentative of their surroundings. Mean filtering is usually thought of as a convolution filter. Like other convolutions it is based around a kernel, which represents the shape and size of the neighborhood to be sampled when calculating the mean. Often a 3×3 square kernel is used, as shown in Figure 1, although larger kernels (e.g. 5×5 squares) can be used for more severe smoothing. (Note that a small kernel can be

applied more than once in order to produce a similar but not identical effect as a single pass with a large kernel.)

$\frac{1}{9}$	$\frac{1}{9}$	$\frac{1}{9}$
$\frac{1}{9}$	$\frac{1}{9}$	$\frac{1}{9}$
$\frac{1}{9}$	$\frac{1}{9}$	$\frac{1}{9}$

Figure 3.2 3×3 averaging kernel often used in mean filtering

D. SUPER PIXEL FEATURE EXTRACTION

This section introduces how to utilize the superpixels to create three feature images, which separately reflect the spectral information and spatial information within and among superpixels. Then, three kernels are computed on the pixels from the feature images to exploit the spectral-spatial information of superpixels. Each superpixel is a group of neighboring spectral pixels y_{zi} , $z = 1, \dots, Z$, which can be transformed into a matrix YSP_i . As described in Section II, spectral pixels representing the spectral information of superpixels in the HSI can be directly used as the spectral feature. All the spectral pixels in the HIS constitute the spectral feature image $ISpec$. To exploit the spatial information within each superpixel, a mean operation is first applied on the spectral pixels $[y_{1i}, \dots, y_{Zi}]$ within each superpixel YSP_i , and then, the mean pixel y_{Meani} is assigned to all pixels in each superpixel. Here, YSP_i is still the superpixel, which consists of a number of spectral pixels. This operation is the same as mean filtering and can reduce the interferences (e.g., noise) in each superpixel. All the filtered superpixels can constitute a mean feature image $IMean$. Note that adopting other more powerful filtering approaches (e.g., guided filtering and nonlocal filtering) might enhance the performance but increase the computational cost.

Weighted Average Filtering

The weighted mean filtering has been applied widely as an advanced method compared with standard mean filtering. The weighted mean filtering performs spatial processing to determine which pixels in an image have been affected by impulse noise. The weighted mean filtering classifies pixels as noise by comparing each pixel in the image to its surrounding neighbor pixels. The size of the neighborhood is adjustable, as well as the threshold for the comparison. A pixel that is different from a majority of its neighbors, as well as being not structurally aligned with those pixels to which it is similar, is labeled as impulse noise. These noise pixels are then replaced by the median pixel value of the

pixels in the neighborhood that have passed the noise labeling test.

Purpose

- 1). Remove impulse noise
- 2). Smoothing of other noise
- 3). Reduce distortion, like excessive thinning or thickening of object boundaries

E. FEATURE SELECTION

In machine learning and statistics, feature selection, also known as variable selection, attribute selection or variable subset selection, is the process of selecting a subset of relevant features (variables, predictors) for use in model construction. Feature selection techniques are used for three reasons:

- Simplification of models to make them easier to interpret by researchers/users,
- Shorter training times,
- Enhanced generalization by reducing over fitting (formally, reduction of variance).

The central premise when using a feature selection technique is that the data contains many features that are either redundant or irrelevant, and can thus be removed without incurring much loss of information. Redundant or irrelevant features are two distinct notions, since one relevant feature may be redundant in the presence of another relevant feature with which it is strongly correlated. Feature selection techniques should be distinguished from feature extraction. Feature extraction creates new features from functions of the original features, whereas feature selection returns a subset of the features. Feature selection techniques are often used in domains where there are many features and comparatively few samples (or data points). Archetypal cases for the application of feature selection include the analysis of written texts and DNA microarray data, where there are many thousands of features, and a few tens to hundreds of samples.

F. PARTICLE SWARM OPTIMIZATION

Particle Swarm Optimization is an approach to problems whose solutions can be represented as a point in an n-dimensional solution space. A number of particles are randomly set into motion through this space. At each iteration, they observe the "fitness" of themselves and their neighbours and "emulate" successful neighbours (those whose current position represents a better solution to the problem than theirs) by moving towards them. Various schemes for grouping particles into competing, semi-independent flocks can be used, or all the particles can belong to a single global flock. This extremely simple approach has been surprisingly effective across a variety of problem domains.

PSO was developed by James Kennedy and Russell Eberhart in 1995 after being inspired by the study of bird flocking behaviour by biologist Frank Heppner. It is related to evolution-inspired problem solving techniques such as genetic algorithms.

G. SUPPORT VECTOR MACHINE CLASSIFICATION

In machine learning and statistics, classification is the problem of identifying to which of a set of categories (sub-populations) a new observation belongs, on the basis of a training set of data containing observations (or instances) whose category membership is known.

An example would be assigning a given email into "spam" or "non-spam" classes or assigning a diagnosis to a given patient as described by observed characteristics of the patient (gender, blood pressure, presence or absence of certain symptoms, etc.). Classification is an example of pattern recognition.

In the terminology of machine learning,[1] classification is considered an instance of supervised learning, i.e. learning where a training set of correctly identified observations is available. The corresponding unsupervised procedure is known as clustering, and involves grouping data into categories based on some measure of inherent similarity or distance.

IV - SIMULATION RESULTS

This section displaying the results obtained for the University pavia images and the total number of spectral bands of are 103. The following figure depicts the various spectral bands of Pavia images, the image are clearly describing the visible spectrum variation is each band of interest.

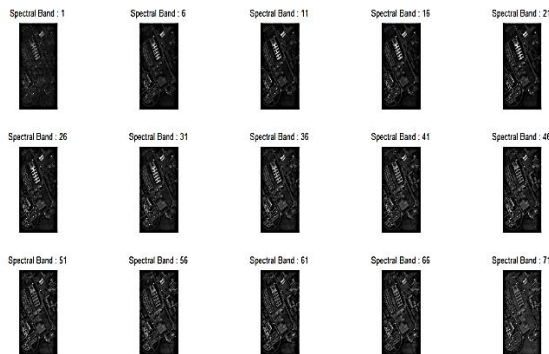


Figure 7.3 various spectral bands of Pavia image

The principal component analysis is applied on the whole spectral band images (103). The first three principal component vectors are considered for the super pixel segmentation. The following figure represents the three principal components obtained for the Pavia images.

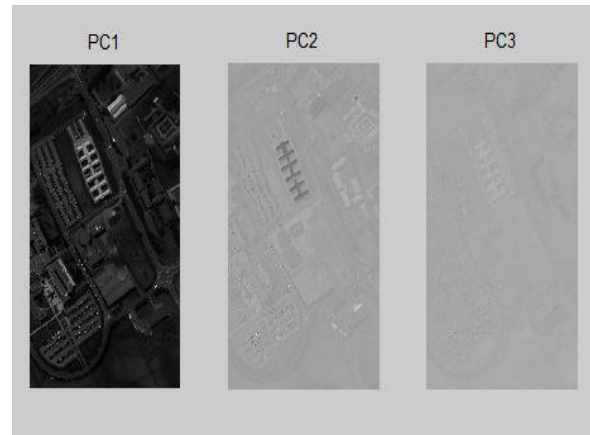


Figure 7.4 three principal component images

The super pixel segmentation results obtained for the proposed work is shown in the following figure.



Figure 7.5 Super pixel segmentation result

The mean filtered spectral band are shown in the following figure where the randomly selected 25 coordinates are used for the feature extraction. The figure 7.6 and 7.7 are depicts the mean and weighted average filtered Pavia images.



Figure 7.6 Mean filtered Pavia images

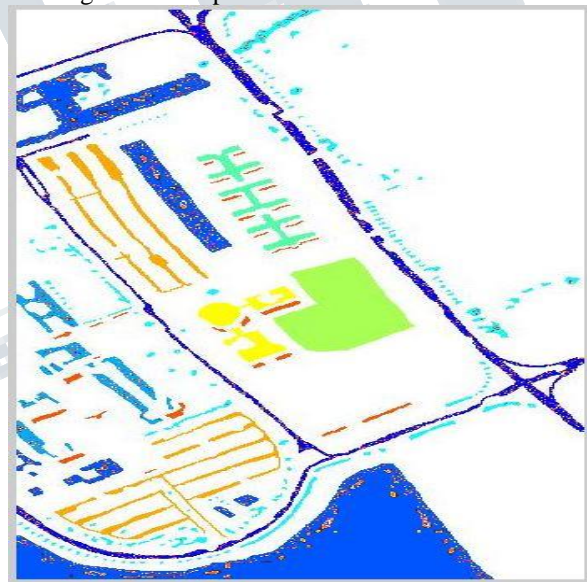
The mean feature extracted from the Pavia images are compared with the various filtering technique. The following table represents the various filtering features

Super pixel No.	Mean filtering	Weighted Mean filtering	Gaussian filtering
1	28.4534	0.1915	52
2	34.8635	0.4845	54
3	20.7445	0.4335	42
4	36.9043	0.5100	80
5	37.1127	0.4891	95

The output obtained from the proposed work is shown in the following figure. The Pavia images are having the 9 classes as final segmented output.



Figure 7.7 Weighted Mean filtered Pavia images



- Asphalt
- Meadows
- Gravel
- Trees
- Metal sheets
- Bare soil
- Bitumen
- Bricks
- Shadows

Figure 7.8 Final segmentation result for Pavia images

V - CONCLUSION

In this project, we present a super pixel based segmentation method for HSI classification. Instead of using a fixed-size region as some previous works, this work adopts the superpixel, whose size and shape can be adaptively adjusted according to the spatial structures of the HSI. Then, the particle swarm optimization algorithm used for the optimum feature selection effectively exploit the spectral-spatial information within and among superpixels. The experimental results on three real HSI images demonstrate the superiority of the proposed PSO based SVM classifier over several well-known classifiers, in terms of both visual quality on the classification map and quantitative metrics. The proposed work is implemented on MATLAB R2014a software and the obtained results are showing the effectiveness of the proposed work.

REFERENCES

- [1] J. Li, J. M. Bioucas-Dias, and A. Plaza, "Spectral-spatial hyperspectral image segmentation using subspace multinomial logistic regression and Markov random fields," *IEEE Trans. Geosci. Remote Sens.*, vol. 50, no. 3, pp. 809–823, Mar. 2012.
- [2] D. Böhning, "Multinomial logistic regression algorithm," *Ann. Inst. Stat. Math.*, vol. 44, no. 1, pp. 197–200, Mar. 1992.
- [3] F. Melgani and L. Bruzzone, "Classification of hyperspectral remote sensing images with support vector machines," *IEEE Trans. Geosci. Remote Sens.*, vol. 42, no. 8, pp. 1778–1790, Aug. 2004.
- [4] M. Fauvel, Y. Tarabalka, J. A. Benediktsson, J. Chanussot, and J. C. Tilton, "Advances in spectral-spatial classification of hyperspectral images," *Proc. IEEE*, vol. 101, no. 3, pp. 652–675, Mar. 2013.
- [5] L. Zhang, L. Zhang, D. Tao, and X. Huang, "Sparse transfer manifold embedding for hyperspectral target detection," *IEEE Trans. Geosci. Remote Sens.*, vol. 52, no. 2, pp. 1030–1043, Feb. 2014.
- [6] J. Li, J. M. Bioucas-Dias, and A. Plaza, "Spectral-spatial hyperspectral image segmentation using subspace multinomial logistic regression and Markov random fields," *IEEE Trans. Geosci. Remote Sens.*, vol. 50, no. 3, pp. 809–823, Mar. 2012.
- [7] B. Du and L. Zhang, "Target detection based on a dynamic subspace," *Pattern Recog.*, vol. 47, no. 1, pp. 344–358, Jan. 2014.
- [8] Y. Chen, N. M. Nasrabadi, and T. D. Tran, "Hyperspectral image classification using dictionary-based sparse representation," *IEEE Trans. Geosci. Remote Sens.*, vol. 49, no. 10, pp. 3973–3985, Oct. 2011.
- [9] U. Srinivas, Y. Chen, V. Monga, N. M. Nasrabadi, and T. D. Tran, "Exploiting sparsity in hyperspectral image classification via graphical models," *IEEE Geosci. Remote Sens. Lett.*, vol. 10, no. 3, pp. 505–509, May 2013.
- [10] J. Li, J. M. Bioucas-Dias, and A. Plaza, "Semisupervised hyperspectral image segmentation using multinomial logistic regression with active learning," *IEEE Trans. Geosci. Remote Sens.*, vol. 48, no. 11, pp. 4085–4098, Nov. 2010.